Direct Numerical Simulations of Rayleigh-Taylor Instability with Gravity Reversal

Daniel Livescu,
Tie Wei, CCS-2

We present results from an extensive new set of Direct Numerical Simulations (DNS) of Rayleigh-Taylor instability (RTI). The set includes a suite of simulations with grid size of 1024^2 x 4608 and Atwood number ranging from 0.04 to 0.9, in order to examine small departures from the Boussinesq approximation as well as large density ratio effects, and a high resolution simulation of grid size 4096^2 x 4032 and Atwood number of 0.75, which is the largest instability simulation to date. After the layer width had developed substantially, additional branched simulations have been run under reversed and zero gravity conditions. These simulations represent unit problems for the variable acceleration case encountered in practical applications. While the bulk of the results is still being analyzed, here we focus on the modifications in the mixing layer structure and turbulence in response to the acceleration change [1].

Although RTI has been subjected to intense research over the last 50 years, until recently numerical studies have been restricted to coarse mesh calculations. On the other hand, it is notoriously difficult in laboratory experiments to accurately characterize and control the initial conditions and provide the detailed measurements needed for turbulence model development and validation. Thus, a large number of open questions remain unanswered about this instability and even first-order global quantities, such as the layer growth, are not completely understood and still give rise to intense debate [2,3]. Nevertheless, today's petascale computers allow fully resolved simulations of RTI at parameter ranges comparable to those attained in laboratory experiments, but providing, in carefully controlled initial and boundary conditions studies, much more information than physical experiments. These extremely high resolution simulations are enabling a look at the physics of turbulence and turbulent mixing in unprecedented detail, hopefully contributing to a significant advance in our understanding of these phenomena [4].

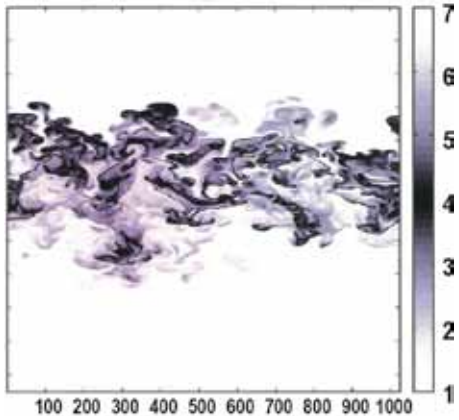

Fig. 1. 2D snapshot of the mixing layer from the forward gravity case at the reference time.

Although in many instances, for example in atmospheric or oceanic flows, the acceleration may be considered as constant, there are important practical applications where the driving acceleration changes in time and may even reverse sign. Some examples include Inertial Confinement Fusion (ICF), supernovae, and pulsating stars. RTI with complex acceleration history, including changes in sign, have been studied both experimentally and in coarse mesh numerical simulations; however, much less is known about the physics of the flow compared to the classical RTI. In addition, most engineering turbulence models cannot capture the change in the mixing layer behavior following gravity reversal. In order to better understand the variable acceleration effects on the instability development and turbulence properties, we have proposed two unit problems: reversing or setting the acceleration to zero in the turbulent stage of the classical RTI [5]. The latter is related to the Richtmyer-Meshkov instability, when the two fluids are subjected to an impulsive acceleration, for example, due to a shock wave.

All simulations have been performed with the CFDNS code [6]. We have carried out extensive resolution studies to ensure that the solution is converged and all flow scales are accurately resolved. While the bulk of the results are still being analyzed, we present here, preliminary results from three simulations, with A = 0.75, representing classical, reversed, and zero gravity RTI cases.

The primary nondimensional parameter characterizing differential acceleration effects is the Atwood number, $A = (\rho_h-\rho_l)/(\rho_h+\rho_l)$, where ρ_l, ρ_h are densities of the light and heavy fluids, respectively. The Atwood number ranges from 0 to 1. For air inter-penetrating helium, for which the density ratio is 7, the Atwood number is A = 0.75. For air and hydrogen, A = 0.85.

In contrast, the Boussinesq approximation corresponds to A -> 0 and a value of 0.05 is usually taken to define this limit. To the best of our knowledge the new set of DNS addressed here is the first to consider A > 0.5. Yet the development of the instability and the mixing itself are fundamentally different at high and low A [2]. For example, our previous results in an idealized triply-periodic buoyancy-driven flow show that the mixing is asymmetric at large density ratios, with the pure light and heavy fluids mixing at different rates [7,8]. We refer to such flows as variable-density (VD) flows.

For more information contact Daniel Livescu at livescu@lanl.gov.

Funding Acknowledgments
DOE, NNSA, Defense Science Programs, Weapons Science Campaigns

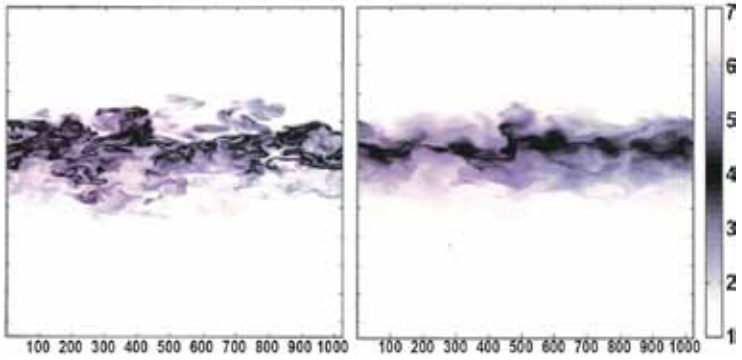

Fig. 2. 2D snapshot of the mixing layer from the reversed gravity case at the (left) reference time and (right) late time.

The change in the structure of the mixing layer after the gravity reversal can be clearly seen in Figs. 1 and 2. In the forward gravity case (Fig. 1), the interpenetration of the two fluids is highly irregular, giving rise to local density inversions, similar to the previous lower A results [9]. These inversions are quickly removed as the buoyancy force reverses sign so that, at late times, the stratification becomes relatively uniform across the layer (Fig. 2). On the contrary, if the gravity is set to zero, the local structures are preserved (not shown here). As the layer continues to grow due to the inertia of the individual fluid parcels, the instability still develops and the constant density surfaces become even more corrugated. This is similar to the post re-shock evolution of the mixing layer in the Richtmyer-Meshkov instability.

Fig. 3. Mean density profiles corresponding to the three cases at the reference and late times.

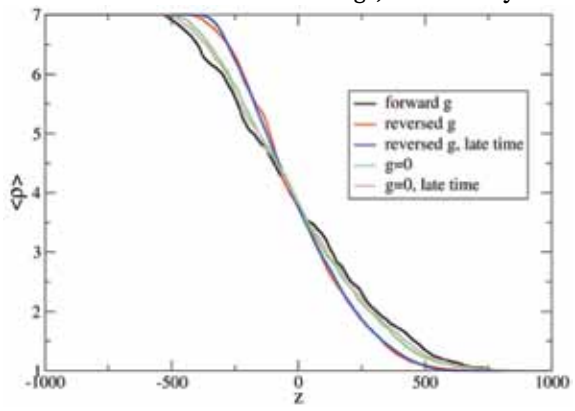

In general, the spectral properties (in terms of fully developed spectra showing the emergence of an inertial range) and vorticity and density gradient alignments with the strain tensor eigenvectors remain similar, following the change in gravity, with the forward density case and with the usual canonical turbulent flows. However, for the reversed gravity case, the vector quantities enumerated above also acquire a strong directionality with the coordinate directions. In addition, gravity reversal efficiently mixes the largescales in the inner region of the layer, so that the large-scale anisotropy decreases to zero and the stratification becomes uniform across the layer. However, the anomalous small-scale anisotropy associated with buoyancy-driven turbulence [2,9] is actually increased by gravity reversal.

On the other hand, the mean density profiles shown in Fig. 3 give little indication of the dramatic modifications in the underlying density field structure as the gravity changes. However, these modifications have a significant influence on the turbulence transport, rendering the popular gradient diffusion hypothesis, used in moment closures, not appropriate. For example, the mass flux is closed in two-equation models like **k-L** or **k**-ε as proportional to the mean density gradient. Figure 4 shows that the mass flux changes considerably (even reverses sign) following the gravity reversal, which clearly cannot be captured by a gradient diffusion hypothesis. Thus two-equation models cannot capture such flows; one needs a separate mass flux transport equation, as it is done, for example, in the BHR model [10].

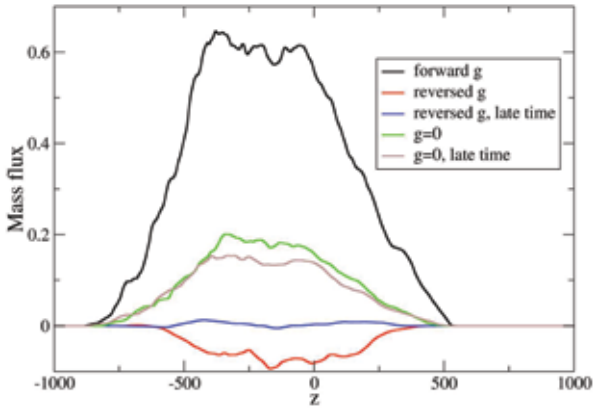

Fig. 4. Mass flux variation across the layer for the three cases at the reference and late times.

[1] Livescu, D. and T. Wei, *Proceedings 7th International Conf Comput Fluid Dynam,* (ICCFD7), 2304 (2012).

[2] Livescu D. et al., *Phys Scripta* **T142**, 014015 (2010).

[3] Dimonte G. et al., *Phys Fluids* **16,** 1668 (2004).

[4] Livescu, D. et al., "Numerical simulations of Two Fluid Turbulent Mixing at Large Density Ratio and Applications to the Rayleigh-Taylor Instability," *R. Soc London Phil Trans. A* (to appear).

[5] Livescu, D. et al., *J Phys Conf Ser* **318,** 082007 (2011).

[6] Livescu, D. et al., "CFDNS: A Computer Code for Direct Numerical Simulations of Turbulent Flows," LA-CC-09-100.

[7] Livescu, D. and J. R. Ristorcelli, *J Fluid Mech* **591,** 43 (2007).

[8] Livescu, D. and J. R. Ristorcelli, *J Fluid Mech* **605,** 145 (2008).

[9] Livescu, D. et al., *J Turbul* **10,** 1 (2009).

[10] Schwarzkopf, J. D. et al., *J Turbul* **12,** 1 (2011).